Published in final edited form as:
CNS Neurol Disord Drug Targets. 2013 May 1; 12(3): 338–349.

Age-dependent microglial activation in immature brains after hypoxia-ischemia

Peter Ferrazzano[1,3,*], **Vishal Chanana**[3], **Kutluay Uluc**[1,2], **Emin Fidan**[1], **Erinc Akture**[2], **Douglas B. Kintner**[1], **Pelin Cengiz**[1,3], and **Dandan Sun**[4]

[1]Dept. of Pediatrics, University of Wisconsin School of Medicine and Public Health, Madison, WI 53705

[2]Dept. of Neurological Surgery, University of Wisconsin School of Medicine and Public Health, Madison, WI 53705

[3]Waisman Center, University of Wisconsin School of Medicine and Public Health, Madison, WI 53705

[4]Dept. of Neurology, University of Pittsburgh, Pittsburgh, PA 15213

Abstract

In the present study, we tested whether the ongoing differentiation of microglia in the immature brain results in more robust microglial activation and pro-inflammatory responses than juvenile brains following hypoxia-ischemia (HI). Under normoxic conditions, microglial activation profiles were assessed in postnatal day 9 and postnatal day 30 mice (P9 and P30) by analyzing relative expression levels of CD45 in $CD11b^+/CD45^+$ microglia/macrophages. Flow cytometry analysis revealed that the hippocampi of P9 and P30 brains exhibited higher levels of CD45 expression in $CD11b^+/CD45+$ cells than in the cortex and striatum. In response to HI, there was an early increase in number of $CD11b^+/CD45^+$ microglia/macrophages in the ipsilateral hippocampus of P9 mice. These cells transformed from a “ramified” to an “amoeboid” morphology in the CA1 region, which was accompanied by a loss of microtubule-associated protein 2 immunostaining in this brain region. The peak response of microglial activation in the ipsilateral hippocampus of P9 mice occurred on day 2 post-HI, which was in contrast to a delayed and persistent microglial activation in the cortex and striatum (peak on day 9 post-HI). P9 brains demonstrated a 2–3 fold greater increase in microglia counts than P30 brains in each region (hippocampus, cortex, and striatum) during day 1–17 post-HI. P9 brains also showed more robust expression of pro-inflammatory cytokines (tumor necrosis factor-alpha, interleukin-1β) than P30 brains. Taken together, compared to P30 mice, P9 mice demonstrated differences in microglial activation and pro-inflammatory responses after HI, which may be important in brain damage and tissue repair.

Keywords

microglia; neonatal hypoxic ischemia; inflammation; apoptosis

INTRODUCTION

In contrast to the adult brain, microglia in the healthy immature brain are activated, phagocytic cells responsible for removal of cellular debris that occurs during normal brain

[*]Address correspondence to: Peter Ferrazzano, M.D., Department of Pediatrics, University of Wisconsin Medical School, T517 Waisman Center, 1500 Highland Ave., Madison, WI, 53705, Tel: (608) 890-0759, Fax: (608) 263-1409, ferrazzano@pediatrics.wisc.edu.

development [1]. Microglia are also important in promotion of axonal growth and neuronal differentiation and angiogenesis in developing brains [2, 3]. These activated microglia are abundant in white matter tracts, and have been implicated in the characteristic susceptibility to white matter injury in premature infants suffering from perinatal asphyxia [4]. In early infancy microglia transition from a reactive phagocyte to ramified immunosurveillance cell, a state maintained throughout adulthood [5]. Recent studies have shown that these "surveying" microglia are extremely dynamic and play a role in neuroplasticity through phagocytosis of synaptic structures during adult neurogenesis, active remodeling of the perisynaptic environment, and the release of soluble factors [6].

Neuroinflammation plays an important role in ischemic brain injury, and modulating the microglia-mediated inflammatory response to ischemia has been considered as a potential target for neuroprotective intervention. Ischemic insult to the developing brain triggers microglia activation, proliferation, and secretion of inflammatory cytokines and chemokines [5, 7, 8], which may be neurotoxic and worsen injury. However, recent research highlights the importance of microglia in promoting neuronal survival and brain repair after ischemia by secretion of anti-inflammatory cytokines and growth factors [9]. It remains unclear whether these contrasting microglial responses to injury vary with neurodevelopment in immature brains.

In the current study, we determined microglial activation in brains of P9 (immature) and P30 (juvenile) mice under normoxic control conditions as well as at days 1–17 post hypoxia ischemia (HI). We found that microglia in the hippocampus of P9 and P30 mice exhibited a more activated microglia phenotype under normoxic conditions. P9 brains exhibited a vigorous pro-inflammatory microglial response after HI, most notably in the hippocampus early after injury. In contrast, less intense microglia activation and proliferation were detected in P30 mice. Therefore, these differential responses may play a role in immature brain injury and repair after HI.

MATERIALS AND METHODS

Materials

Mouse monoclonal anti-microtubule associated protein 2 (MAP2) antibody was from Sigma (St. Louis, MO). Monoclonal rat anti-mouse cluster of differentiation molecule 11b (CD11b) antibody and rat anti-mouse CD45-FITC antibody were from AbD Serotec (Raleigh, NC). Mouse CD11b- APC conjugated antibody, ToPro-3 iodide, goat anti-mouse, Alexa Fluor 488-conjugated IgG and goat anti-rabbit Alexa Fluor 546-conjugated IgG were from Invitrogen (Carlsbad, CA). Vectashield mounting medium were from Vector Labs (Burlingame, CA). Tissue-Tek O.C.T. compound was from Sakura Finetek (Torrance, CA). Hanks balanced salt solution (HBSS) was obtained from Mediatech Cellgro (Manassas, VA). ELISA kits (DuoSet ELISA) for cytokines and cleaved caspase-3 measurements were purchased from R&D Systems (Minneapolis, MN).

Animal usage

All procedures on animals were carried out in adherence with NIH Guide for the Care and Use of - Laboratory Animals and approved by the Institutional Animal Care and Use Committee at the University of Wisconsin-Madison.

Induction of neonatal HI

C57BL/6J mice (P9 and P30) were anesthetized with isoflurane (3% for induction, 1.5% for maintenance), in 30% O_2 and 70% N_2. Since isoflurane has been shown to induce neurotoxicity, we kept the duration of anesthesia to less than 5 min in each animal,

minimizing any potential effects of isoflurane on neuronal injury or microglial activation [10, 11, 12]. The body temperature of the animal was maintained at 37°C with a heating pad. Under a surgical microscope, a midline skin incision was made and the left common carotid artery was electrically cauterized as described before [13]. The incision was rinsed with 0.5% bupivacaine and sutured with a 6.0 prolene suture. Animals were returned to their dams and monitored continuously for 30 min during a 2-hour (h) recovery period. To induce ipsilateral ischemic injury, the animals were placed in a hypoxia chamber (BioSpherix Ltd, Redfield, NY) equilibrated with 10% O_2 and 90% N_2 at 37°C for 50 min. In this model, the unilateral carotid artery ligation itself induces no injury, as perfusion is maintained through collateral circulation. However, on subsequent exposure to hypoxia a hemispheric ischemia occurs as blood flow preferentially decreases to the ligated hemisphere [14]. After HI, animals were monitored continuously for 30 min and then checked every 30 min for 2 h and then daily until sacrificed.

Flow cytometry analysis of brain microglia cells

At day 1–17 after HI, mice were deeply anesthetized with 5% isoflurane plus N_2O and O_2 (3: 2) and decapitated. Immediately after decapitation, cerebellums were removed and meninges were cleaned. The contralateral and ipsilateral hemispheres were separated, and the hippocampus, cortex and striatum were dissected from each hemisphere and submerged into ice-cold HBSS. Samples of each brain region were pooled from 5 mice for analysis. Brain tissues were cut into small pieces and dissociated into a single cell suspension by gentle physical disruption and enzymatic digestion using a commercially available tissue dissociation kit according to manufacturer's instructions (Miltenyi Biotech Inc. Auburn, CA). Myelin was removed by centrifugation of the sample in 0.9M sucrose in HBSS at 2200 g for 10 min at 4°C and cells were rinsed in HBSS and collected after passing through a 40 μm membrane by centrifugation.

For flow cytometry analysis, the cell suspension was first incubated with 10% goat serum in 0.1M PBS (pH 7.4) for 20 min at room temperature. After the incubation, cells were centrifuged at 200 g for 5 min. After aspirating the supernatant, pellet was suspended in fixation buffer (4% paraformaldehyde, million cells/1ml) and incubated for 30 min at room temperature on a rotator. After the incubation, cells were centrifuged at 1000 g for 5 min and washed with 0.1M PBS to remove excess fixation buffer. Fixed cells (10^6 cells) in 0.1 ml PBS were incubated with APC-conjugated rat anti-mouse CD11b and FITC-conjugated rat anti-mouse CD45 antibodies (25 μL of 0.2 mg/ml) for 30 min in ice. Our previous immnunofluorescence staining study with antibodies against two microglial marker proteins CD11b and Iba1 illustrated that these two microglial marker proteins were co-localized in the activated microglia, and indistinguishably exhibited the classical "amoeboid" morphological changes in these cells [15]. Therefore, in the current study, CD11b was chosen to quantify activated microglia, and to characterize microglial/macrophage activation profile by further quantification of CD45 immunofluorescence in the $CD11b^+/CD45^+$ cells with flow cytometry analysis [16, 17, 18]. Cells were rinsed with 0.1M PBS by centrifugation for 5 min at 1000 g and pellets were suspended in 500 μl of 0.1M PBS and acquired immediately with a FACSCalibur flow cytometer running CellQuest Pro software (BD Biosceiences) with the following settings: Forward scatter (FSC) V = E00, gain = 1.0, mode = Lin; Side scatter (SSC) V = 399, gain = 1.25, mode = Lin; FL1 V = 572, gain = 1.0, mode = Log; FL4 V = 704, mode = Log. In each experiment, data with equal number of events (10,000) from contralateral and injured brain regions were acquired for analysis.

Double immunofluorescence staining

Mice were deeply anesthetized with 5% isoflurane plus N_2O and O_2 (3: 2) and transcardially perfused with 0.9% NaCl solution, followed by 4% paraformaldehyde (PFA) in 0.1 M

phosphate-buffered saline (PBS, pH 7.4). Brains were post-fixed in 4% PFA for 12 h, and subsequently cryoprotected with 30% sucrose in 0.1 M PBS for 24–36 h at 4°C. The brains were frozen in Tissue-Tek O.C.T. compound for 10 min and cut into coronal sections (35 μm thickness) on a freezing microtome (Leica SM 2000R; Buffalo Grove, IL), and stored in antifreeze solution at − 20°C. Sections at the level of 0.02 mm posterior from bregma, interaural 3.82 mm; 0.46 mm posterior from bregma, interaural 3.82 mm were selected and processed for immunofluorescence staining [13]. Sections were rinsed in 0.1 M Tris-buffered saline (TBS, pH 7.4) for 15 min, and incubated with a blocking solution (0.1% Triton X-100 and 3% goat serum in 0.1 M TBS) for 30 min at room temperature. To investigate microglial activation and neurodegeneration, sections were then incubated with rat anti-mouse CD11b antibody (1:100) and mouse anti-microtubule- associated protein 2 (MAP2, 1:200) in blocking solution overnight at 4°C. After rinsing with TBS for 30 min, sections were incubated with the following secondary antibodies in blocking solution (1:200) for 1 h at room temperature, according to the primary antibodies recognized: goat anti-rat Alexa Fluor 488-conjugated IgG and goat anti-mouse Alexa Fluor 546-conjugated IgG. After rinsing with TBS for 30 min, sections were incubated with ToPro-3 iodide in blocking solution (1:1000) for 15 min at room temperature. Sections were then mounted on slides with vectashield mounting medium. For negative controls, brain sections were stained with the secondary antibody only.

Fluorescent images were captured on a Leica DMIRE 2 inverted confocal laser-scanning microscope using the Leica confocal software (Leica Microsystems Inc., Buffalo Grove, IL). Samples were excited at 488 nm (argon/krypton), 543 nm and 633 nm, and the emission fluorescence was recorded at 512–548 nm, 585–650 nm, or 650–750 nm, respectively. Identical settings were used to capture the negative control and experimental images.

ELISA for cleaved caspase-3

At 24 h post-HI, mice were anesthetized with 5% isoflurane vaporized in N_2O and O_2 (3: 2) and decapitated. The contralateral and ipsilateral hemispheres were separated and the hippocampus, cortex and deep brain regions were dissected from each hemisphere. Samples of each brain region were pooled from 5 mice for analysis. Brain tissues were cut into small pieces in a PBS buffer containing phosphatase and protease inhibitors as described previously [15]. Brain tissues were gently homogenized with a tissue pestle grinder (Kontes, Vineland, NJ) for 10 strokes in 1 ml of the PBS buffer. The resulting suspension was sonicated with an ultrasonic cell disrupter (Thermo-Fisher Scientific, Waltham, MA) and subjected to two freeze-thaw cycles to further disrupt the cell membranes. The homogenates were centrifuged at 5,000 g at 4°C for 5 min and supernatants were collected for analysis of cleaved caspase-3 using ELISA kit. The total protein concentration of each homogenate was determined using the bicinchoninic acid method. The capture antibody (2.0 μg/ml) was diluted to the working concentration in PBS. 96-well plates were coated overnight with 100 μl per well of the diluted capture antibody. After three washings with wash buffer (0.05% tween 20 in PBS, pH 7.2), plates were blocked by a block buffer (300 μl of 1% BSA and 0.05 % NaN_3 in PBS) for 1 h. Then, 100 μl standards, or homogenate samples (0.6 mg protein) were added and allowed to incubate for 2 h at room temp. After the incubation, 100 μl (150 ng/ml) of the biotinylated detection antibody was added to each well and incubated for 2 h at room temp. 100 μl of the supplied streptavidin-HRP solution (1:200 dilution) was added and plates were allowed to incubate for 20 min. Following washing, chromogen was added. After incubating for 20 min in dark, the reaction was stopped with stop solution. The optical density of each well at 450 nm was determined immediately using a microplate reader (Molecular Devices, Sunnyvale, CA). Concentration of cleaved caspase-3 was calculated with a seven-point standard curve and expressed as pg/mg protein.

ELISA for cytokines

At day 2 or day 9 post-HI, mice were anesthetized with 5% isoflurane vaporized in N_2O and O_2 (3: 2) and decapitated. The contralateral and ipsilateral hemispheres were separated and the hippocampus, cortex and deep brain regions were dissected from each hemisphere. Samples of each brain region were pooled from 5 mice for analysis. Brain tissues were cut into small pieces in a PBS buffer containing phosphatase and protease inhibitors as described previously [15]. Brain tissues were gently homogenized with a tissue pestle for 10 strokes in 1 ml of the PBS buffer. The homogenates were centrifuged at 12,000 g at 4°C for 20 min and supernatants were collected for analysis of TNF-α, IL-1β or IL-10 using ELISA kits. The total protein concentration of each homogenate was determined using the bicinchoninic acid method. The respective capture antibodies were diluted to the working concentration in PBS (TNF-α, 0.8 μg/ml; IL-1β, 4.0 μg/ml; IL-10, 4.0 μg/ml). 96-well plates were coated overnight with 100 μl per well of the diluted capture antibodies. After three washings with wash buffer (0.05% tween 20 in PBS, pH 7.2), plates were blocked by a block buffer (300 μl of 1% BSA in PBS) for 1 h. Then, 100 μl standards, or homogenate samples (0.6 mg protein) were added and allowed to incubate for 2 h at room temp. After the incubation, 100 μl (TNF-α, 200 ng/ml; IL-1β, 600 ng/ml; IL-10, 400 ng/ml) of the biotinylated detection antibodies were added to each well and incubated for 2 h at room temp. 100 μl of the supplied streptavidin-HRP solution (1:200 dilution) was added and plates were allowed to incubate for 20 min. Following washing, chromogen was added. After incubating for 20 min in dark, the reaction was stopped with stop solution. The optical density of each well at 450 nm was determined immediately using a microplate reader. Concentration of TNF-α, IL-1β, or IL-10 was calculated with a seven-point standard curve and expressed as pg/mg protein.

Statistical analysis

Values are expressed as the mean ± SD. Statistical analysis was performed using ANOVA (Bonferroni post-test) to determine group differences (SigmaPlot, Systat Software, San Jose, CA). P-values smaller than or equal to 0.05 were considered statistically significant.

RESULTS

HI triggers accumulation of $CD11b^+/CD45^+$ cells in P9 ischemic brains

We first determined whether HI induced an increase in microglia counts in P9 brain regions. Flow cytometry was used to quantify cells co-expressing the microglia/macrophage surface antigens CD11b and CD45. As shown in Figure 1, flow cytometry scatter plots show two distinct cell populations based on their CD45 and CD11b immunofluorescence staining (Figure 1, A–C). In contralateral brain regions, the majority of cells were CD11b negative and CD45 positive cells ($CD11b^-/CD45^+$), clustered in the lower right quadrants (Figure 1, A–C). These cells most likely represent leukocytes and cellular debris [16, 18]. A small number of $CD11b^+/CD45^+$ microglia/macrophage cells were detected in the contralateral brain regions (upper right quadrants, Figure 1A–C). In contrast, the ipsilateral hippocampus, cortex and striatum showed a large population of $CD11b^+/CD45^+$ cells at day 2 post-HI (hippocampus) or day 9 post-HI (cortex and striatum), (upper right quadrants, Figure 1A–C). These data suggest that HI triggers an increase in microglia/macrophage counts in ipsilateral brain regions of P9 mice.

HI triggers more robust microglia/macrophage response in P9 brains compared to P30

We then monitored changes of the microglia/macrophage population in P9 and P30 brains at days 1–17 following HI. As shown in Figure 2, the $CD11b^+/CD45^+$ cell population remained low (<1000 cell counts) in the contralateral brain regions of P9 brains

(hippocampus, cortex, striatum) post-HI. In contrast, a large increase in the $CD11b^+/CD45^+$ population was detected in the ipsilateral hippocampus (Figure 2A) as early as 1 day post-HI (~2800 cell counts) and peaked at day 2 post-HI (2847 ± 605 cell counts). The $CD11b^+/CD45^+$ cells in the ipsilateral hippocampus then decreased gradually to a low level (< 1000 cells) by one week post-HI (714 ± 16 cell count). This low level was sustained out to day 17 (Figure 2A). P9 ipsilateral cortex exhibited a less dramatic elevation in $CD11b^+/CD45^+$ cell population than in hippocampus. The onset time of the elevation in microglia/macrophage counts was delayed until day 3 post-HI, was muted compared to hippocampus (1563 ± 80 cell count, ~55% of peak hippocampal counts), and was sustained for 12 days post-HI (Figure 2B). By day 17 post-HI, the $CD11b^+/CD45^+$ counts were restored to a low level in the ipsilateral cortex. The ipsilateral striatum of P9 mice demonstrated a distinct time course of microglial response (Figure 2C), with a delayed onset time at day 4 post-HI and peak elevation at day 12 post-HI (~ 3500 cell counts). In contrast, P30 mice demonstrated smaller increases in microglia/macrophage counts while similar regional time-course of microglia responses was seen. A transient elevation of $CD11b^+/CD45^+$ population occurred in the ipsilateral hippocampus of P30 brains at day 2 post-HI (1037 ± 196 cell counts). The ipsilateral cortex and striatum again showed a delayed increase in microglia response, however the increase was milder in P30 mice with peak $CD11b^+/CD45^+$ peak at day 9 post-HI (806 ± 50 and 934 ± 97 cell counts, respectively) and sustained increase out to day 17 post-HI (750 ± 141 and 852 ± 4 cell counts, respectively), (Figure 2A′-C′). Because the microglial responses in P30 brains were not affected dramatically by HI, we only determined $CD11b^+/CD45^+$ cell on day 2, 9, and 17 post-HI. In P30 mice, no microglial activation was detected in the contralateral brain regions throughout the study (Figure 2A′–C′). Figure 2D-D′ summarizes the fold change between ipsilateral and contralateral brain regions at day 2 and day 9 post-HI. The HI-induced increase in $CD11b^+/CD45^+$ cell counts in the hippocampus at day 2 was significantly higher in P9 brains compared to P30 brains. Similarly, the delayed increase in $CD11b^+/CD45^+$ cells at day 9 in cortex and striatum is significantly higher in the P9 brains. Taken together, the data suggests that HI selectively triggers an increase in microglia/macrophage population in the ipsilateral brain regions of P9 brains compared to P30, with an earlier response in hippocampus than in the cortex and striatum.

HI induces increased CD45 expression in microglia/macrophage cells of P9 brains

We then used differential CD45 expression to assess microglial activation state. Resident surveying microglia possess the phenotype $CD11b^+/CD45^{low}$; however, as microglia become activated their CD45 expression is increased to medium or high levels [16, 17, 18]. As shown in Figure 3A–C, the majority of $CD11b^+$ cells in contralateral brain regions of P9 brains showed a low CD45 immunofluorescence intensity (FI) (CD45 FI < 10^2, $CD45^{low}$ population) after HI. This suggests that the contralateral hemispheres contain predominantly surveying microglia population despite the HI treatment. In contrast, HI induced a rightward shift in the CD45 FI histograms of $CD11b^+/CD45^+$ cells (peak FI between $10^2 – 10^3$, a $CD45^{med}$ population) in all 3 ipsilateral brain regions (Figure 3A–C). Moreover, the ipsilateral cortex and striatum in P9 brains exhibited a small population of cells expressing high levels of CD45 (FI > 10^3, a $CD45^{high}$ population), which may represent a small number of phagocytic microglia or invading peripheral macrophages [16]. The summarized data in Figure 3D shows the percentage of the CD11b+/CD45+ cell population with low, medium, or high CD45 expression. The $CD11b^+/CD45^+$ cell population in the contralateral brain regions consists of predominantly $CD45^{low}$ resting microglia (87 ± 6%). P9 mice exposed to HI demonstrated a shift in the $CD11b^+/CD45^+$ cell population to predominantly $CD45^{med}$ reactive microglia (hippocampus 82 ± 4%, cortex 61 ± 4%, striatum 65 ± 6%). In contrast to P9 brains, P30 brains demonstrated less rightward shift in CD45 FI after HI (Figure 3A′–C′). Despite the increased numbers of $CD11b^+/CD45^+$ cells, the microglia/macrophage

population remains predominantly $CD45^{low}$ in all three ipsilateral brain regions of P30 mice after HI (Figure 3D′). These results further suggest that HI triggered more robust microglia/macrophage activation in P9 than in P30 brains. In Figure 3E, E′ we show the regional CD45 FI profile for naïve P9 and P30, respectively. As expected, the microglia/macrophage population was predominantly $CD45^{low}$ in all three regions of P9 and P30 brains. Interestingly, there was a small but significant increase in the level of $CD45^{med}$ reactive microglia in the hippocampus of both P9 and P30 mice.

Immunostaining analysis of HI-mediated microglia/macrophage activation in P9 brains

We further investigated activation of microglia in hippocampus, cortex and striatum in P9 and P30 brains using an immunohistochemistry staining approach. At day 2 post HI, the contralateral hippocampal CA1 region in P9 brains showed a well preserved structure of pyramidal cell layers with abundant expression of MAP2 (arrowhead, Figure 4A, a). In contrast, the ipsilateral hippocampus demonstrated decreased MAP2 expression and disruption of the stratum pyramidale layer structure (open arrowhead, Figure 4A, d). Additionally, many $CD11b^+$ cells were seen in ipsilateral hippocampus. These cells demonstrated an activated morphology with short, stout processes and intense CD11b staining (open arrow, inset in Figure 4A, **e-inset**). On the other hand, despite the loss of MAP2 expression in P30 ipsilateral hippocampus, CD11b immunostaining remained low, and the $CD11b^+$ cells retained the ramified microglia morphology at day 2 post-HI (arrow, Figure 4e′).

Flow cytometry revealed that microglial activation in the cortex and striatum of P9 mice occurred at day 9 post-HI (Figure 3). Therefore, we determined CD11b expression and transformation of microglia morphology in cortex and striatum at this time post-HI. As shown in Figure 4B(a,a′ vs d,d′), a loss of MAP2 occurred in the ipsilateral cortex of both P9 and P30 mice. However, activation of microglial cells was only detected in the ipsilateral cortex in P9 mice (Figure 4B **e-inset**, open arrow). Similar findings were observed in the ipsilateral striatum of P9 mice at day 9 post-HI in Figure 4C (**e-inset**). Taken together, these data suggest that P9 brains respond to HI with a more robust activation of microglia than P30 brains.

Quantification of apoptotic cell death in P9 and P30 brains after HI

To determine whether differential microglia responses were due to possible different intensity of HI lesions, apoptotic cell death was evaluated by quantifying cleaved caspase-3 in three brain regions (hippocampus, cortex and striatum) at 24 hours post-HI using ELISA. As shown in Figure 5, HI induced a significant increase in cleaved caspase-3 in ipsilateral hippocampus of P9 and P30 brains at 24 hours post HI. A smaller but still significant increase in the cleaved caspase-3 was detected in the ipsilateral cortex and striatum of P9 and P30 brains at 24 hours post-HI. There was no significant difference in the cleaved caspase levels of all three regions between P9 and P30. These data suggest that HI induced a similar amount of apoptotic cell death in these two age groups of mice.

HI induces higher pro-inflammatory cytokine expression in P9 than in P30 brains

We next examined whether the robust microglial activation in P9 brains causes stronger pro-inflammatory responses in P9 compared to P30 brains. On day 2 post-HI, the contralateral hemispheres (hippocampus, cortex, striatum) of P9 brains expressed low levels of TNF-α (Figure 6A). In contrast, the ipsilateral hippocampus initially exhibited a transient elevation of TNF-α (277 ± 39 pg/mg protein) at day 2 post-HI, which returned to the contralateral levels at day 9 post-HI (Figure 6A). A similar transient expression pattern for IL1-β (237 ± 20 pg/mg) was also detected in hippocampus (Figure 6B). Interestingly, the anti-inflammatory cytokine IL-10 remained elevated in the hippocampus on day 9 post-HI (90 ±

6 pg/mg on day 2 vs 92 ± 12 on day 9, Figure 6C). Both cortex and striatum in P9 mice exhibited a delayed expression of TNF-α and IL1-β at 9 day post-HI (183 ± 2 pg/mg and 142 ± 11 pg/mg, respectively, Figure 6A, B). The regional (hippocampus, cortex, striatum) and temporal (day 2 vs. day 9 post-HI) pattern of cytokine increases that we observed in P9 brains match the changes seen in microglia proliferation and $CD45^+$ expression (see Figure 2), confirming the activation state of these cells.

In P30 hippocampus, a smaller rise in TNFα (123 ± 18 pg/mg) and IL-1β (138 ± 7 pg/mg) expression compared to P9 brains was demonstrated on day 2 post-HI (Figure 6A′, B′). The increases were ~ 55% and 42% less, respectively, than that in P9 hippocampus. The ipsilateral P30 cortex and striatum also showed a smaller increase in TNF-α and IL-1β expression (Figure 6A′, B′). Interestingly, IL-10 levels were elevated at day 2 in P30 hippocampus at a level similar to the P9 hippocampus, and remained elevated at day 9 post-HI. In P30 cortex and striatum, IL-10 levels were increased at day 9 post-HI (Figure 6C′). Taken together, these results indicate that HI triggers a more robust pro-inflammatory cytokine response in P9 brains compared to P30 brains, which is consistent with the microglial activation profiles in these brains.

DISCUSSION

The role of microglial in the developing brain

Microglia are derived from myeloid precursor cells which invade the brain during early embryonic development [3]. Immature microglia are ameboid, phagocytic cells that phagocytose the cellular debris which occurs during brain development [2, 3]. These ameboid cells migrate through the brain along developing white matter tracts, and spread throughout grey matter regions by 30 weeks of gestation in human fetus [19]. During late fetal development, microglia transition from activated phagocytic cells into a resting immunosurveillance cell with a highly ramified morphology, a process which continues post-natally in humans and rodents [5]. During this transition, microglia remain activated, and play a role in synaptic pruning, neuronal differentiation, and astrocytic proliferation [2, 3]. The activated phenotype and preferential location in developing white matter tracts suggest that microglia may contribute to the characteristic white matter injury which occurs after perinatal ischemia [20]. Regional variations within the developing brain in the time-course of microglial down-regulation are poorly understood.

In this study, we first investigated regional differences in baseline activation state of microglia in P9 and P30 brains. We found increased CD45 expression in hippocampus of both P9 and P30 mice, suggesting a more activated microglial phenotype in this region. This activated microglia phenotype may be related to ongoing synaptic remodeling or neurogenesis in the hippocampus. It has been shown that neurogenesis in the subgranular zone of the dentate gyrus is associated with microglial phagocytosis of apoptotic neuroprogenitor cells throughout the first year of life in mice [21], and mice deficient in the microglial fractalkine receptor demonstrate decreased hippocampal microglia, deficient synaptic pruning, and persistence of immature brain circuitry [2]. Interestingly, we found that this regional increase in baseline microglia activation state in the hippocampus correlated with an early increase in microglia activation and proliferation after HI in both P9 and P30 mice.

HI triggers more microglial activation and pro-inflammatory cytokine release in P9 compared to P30 brains

A number of studies have shown that HI results in proliferation of resident microglia and migration of microglia into denervated zones, with variable contribution from blood-derived

macrophages [22, 23, 24, 25, 26, 27]. In the current study we investigated whether the microglial response is influenced by the age at which injury occurs. We found that HI triggers a much larger increase in microglia counts in P9 ipsilateral brain regions than in P30 mice. This finding is consistent with the report of greater BrdU labeled microglial in P9 cortex compared to P21 mice after HI [28]. These data suggest that the expansion of $CD11b^{+}/CD45^{+}$ cells after HI is largely due to microglial proliferation.

We characterized CD45 expression profiles to further investigate microglial activation state after HI and to differentiate reactive microglia from invading peripheral monocytes. Blood-borne macrophages and parenchymal cells of monocytic lineage (including quiescent or activated resident brain microglia) can be distinguished in rodent brains based on differential CD45 expression levels: $CD45^{high}$ expression levels in blood-born monocytes, in contrast to $CD45^{low}$ expression in quiescent microglial and $CD45^{medium}$ expression levels in activated microglia [16, 17, 18, 29]. We found that expansion of the microglia population after HI in P9 mice was accompanied by a shift to a predominantly activated $CD45^{med}$ profile. At day 2 post-HI, there was a marked increase in $CD11b^{+}/CD45^{med}$ expressing cells in P9 hippocampus, while no increase in $CD11b^{+}/CD45^{high}$ macrophages was detected. These results imply that the early inflammatory response to HI in P9 mice consists of activation and proliferation of microglia rather than invasion of peripheral monocytes. This is in agreement with the finding that the macrophage population is derived from resident microglia rather than peripheral monocytes after neonatal stroke [16]. However, we did find a small population of $CD11b^{+}/CD45^{high}$ cells in the P9 cortex and striatum at post-HI day 9, suggesting that peripheral macrophage invasion may occur late after HI.

In contrast, P30 mice retained a predominantly resting $CD45^{low}$ profile after HI. We did not detect any $CD11b^{+}/CD45^{high}$ cells in any brain region at any time-point in P30 mice, suggesting that peripheral macrophage invasion may not play an important role in the inflammatory response to HI at this age. Invasion of peripheral monocytes into injured tissue frequently accompanies breakdown of the blood-brain barrier [30]. Age-dependent differences in the integrity of the blood-brain barrier, and its susceptibility to breakdown after injury have been described previously and may account for the greater contribution of peripheral macrophages to the late inflammatory response to HI in immature brains [5, 31].

In this study, we chose to expose P9 and P30 mice to the same duration of hypoxic exposure to evaluate age-dependent differences in the microglial response to HI. Age and strain dependent differences in susceptibility to HI have been described, and the microglial response varies with severity of injury [32, 33]. In order to determine whether the 50 minute of 10% O_2 exposure in this study indeed produced a similar degree of insult in P9 and P30 mice, we measured apoptotic cell death at 24 hours post-HI. Both p9 and p30 mice exhibited significant cleavage of caspase-3 at 24 h of HI and we did not detect any difference in all three tested brain regions between P9 and P30 mice. Taken together, these data suggest that the lessened microglial activation in P30 mice is not due to milder apoptotic cell death in these mice.

Our assessment of pro- and anti-inflammatory cytokines after HI provides additional insight into age-dependent differences in the microglial response to HI. We found an early increase in the inflammatory cytokines in the hippocampus of P9 and P30 mice, and a delayed increase in in cortex and striatum. This regional time-course of cytokine release parallels the profile of microglial activation in our flow cytometry analysis. Interestingly, TNF-α and IL-1b levels were ~2–3 fold higher in P9 mice compared to P30 mice. Additionally, in P30 mice the pro-inflammatory cytokine expression was balanced by a comparable increase in expression of the anti-inflammatory cytokine IL-10. IL-10 is a pleiotropic CNS cytokine which limits macrophage accumulation and can reverse IL-1b and TNF-α mediated

excitotoxic injury when administered exogenously [34]. In summary, our data demonstrate that the microglial response to HI in P9 brains is characterized by vigorous microglial activation and a predominantly pro-inflammatory cytokine response, while P30 brains exhibit less microglial activation and a more balanced pro- vs. anti- inflammatory response.

Implications of age-dependent microglial responses on targeting the neuroinflammatory response for neuroprotective strategies after HI

Microglia have a dual function after ischemia. On the one hand, microglia respond to injury by activation and proliferation, and secretion of pro-inflammatory cytokines, chemokines, and reactive oxygen species. These inflammatory mediators are toxic to neurons, astrocytes, oligodendrocytes and endothelial cells, worsening injury [35, 36, 37]. On the other hand, microglia also secrete growth factors and anti-inflammatory mediators which may support neuronal differentiation and survival after injury [38, 39]. In addition, microglial phagocytosis of cellular debris after injury is important for remyelination [40]. Therefore, therapeutic strategies which limit the cytotoxic microglial response and/or augment the regenerative response hold great potential for improving outcomes after HI.

CONCLUSIONS

Our findings of differential microglial responses to HI in P9 and P30 mice suggest that age-dependent differences in microglial responses may impact the efficacy of anti-inflammatory treatment strategies after HI. The P9 brains demonstrated a dramatic increase in microglia activation and a predominantly pro-inflammatory cytokine response early after HI, suggesting that inhibition of microglia may provide benefit in immature brains when administered soon after injury. In contrast, despite similar levels of apoptotic cell death early after injury, the P30 mice demonstrated less microglia activation and a more balanced pro- vs. anti- inflammatory response after HI, suggesting that inhibition of microglia in juvenile brains may be less effective or possibly worsen the outcome after HI. Future studies are needed to assess the impact of age-dependent microglial responses on the neuroprotective efficacy and therapeutic window of microglial inhibition after HI.

Acknowledgments

The authors would like to thank Sonalee Barthakur for assistance with immunofluorescence staining. This work was in part supported by UL1TR000427 from the Clinical and Translational Science Award program of NCATS and NIH (P. Ferrazzano), NIH grants RO1NS048216 and R01NS038118 (D. Sun), and NIH grant P30 HD03352 (Waisman Center).

LIST OF ABBREVIATIONS

CL	contralateral
IL-1β	interleukin-1β
IL-10	interleukin-10
IL	ipsilateral hemispheres
HBSS	Hanks balanced salt solution
HI	hypoxia ischemia
MAP2	microtubule associated protein 2
TNF-α	tumor necrosis factor-alpha

References

1. Graeber MB, Streit WJ. Microglia: Biology and pathology. Acta neuropathologica. 2010; 119(1): 89–105. [PubMed: 20012873]
2. Paolicelli RC, Bolasco G, Pagani F, Maggi L, Scianni M, Panzanelli P, Giustetto M, Ferreira TA, Guiducci E, Dumas L, Ragozzino D, Gross CT. Synaptic pruning by microglia is necessary for normal brain development. Science. 2011; 333(6048):1456–1458. [PubMed: 21778362]
3. Czeh M, Gressens P, Kaindl AM. The yin and yang of microglia. Dev Neurosci. 2011; 33(3–4):199–209. [PubMed: 21757877]
4. Billiards SS, Haynes RL, Folkerth RD, Trachtenberg FL, Liu LG, Volpe JJ, Kinney HC. Development of microglia in the cerebral white matter of the human fetus and infant. The Journal of comparative neurology. 2006; 497(2):199–208. [PubMed: 16705680]
5. Vexler ZS, Yenari MA. Does inflammation after stroke affect the developing brain differently than adult brain? Dev Neurosci. 2009; 31(5):378–393. [PubMed: 19672067]
6. Tremblay ME, Stevens B, Sierra A, Wake H, Bessis A, Nimmerjahn A. The role of microglia in the healthy brain. J Neurosci. 2011; 31(45):16064–16069. [PubMed: 22072657]
7. Biran V, Joly LM, Heron A, Vernet A, Vega C, Mariani J, Renolleau S, Charriaut-Marlangue C. Glial activation in white matter following ischemia in the neonatal p7 rat brain. Experimental neurology. 2006; 199(1):103–112. [PubMed: 16697370]
8. Deng W. Neurobiology of injury to the developing brain. Nat Rev Neurol. 2010; 6(6):328–336. [PubMed: 20479779]
9. Lalancette-Hebert M, Gowing G, Simard A, Weng YC, Kriz J. Selective ablation of proliferating microglial cells exacerbates ischemic injury in the brain. The Journal of neuroscience: the official journal of the Society for Neuroscience. 2007; 27(10):2596–2605. [PubMed: 17344397]
10. Zhang Y, Xu Z, Wang H, Dong Y, Shi HN, Culley DJ, Crosby G, Marcantonio ER, Tanzi RE, Xie Z. Anesthetics isoflurane and desflurane differently affect mitochondrial function, learning, and memory. Ann Neurol. 2012; 71(5):687–698. [PubMed: 22368036]
11. Wu X, Lu Y, Dong Y, Zhang G, Zhang Y, Xu Z, Culley DJ, Crosby G, Marcantonio ER, Tanzi RE, Xie Z. The inhalation anesthetic isoflurane increases levels of proinflammatory tnf-alpha, il-6, and il-1beta. Neurobiol Aging. 2012; 33(7):1364–1378. [PubMed: 21190757]
12. Xie Z, Culley DJ, Dong Y, Zhang G, Zhang B, Moir RD, Frosch MP, Crosby G, Tanzi RE. The common inhalation anesthetic isoflurane induces caspase activation and increases amyloid beta-protein level in vivo. Ann Neurol. 2008; 64(6):618–627. [PubMed: 19006075]
13. Cengiz P, Kleman N, Uluc K, Kendigelen P, Hagemann T, Akture E, Messing A, Ferrazzano P, Sun D. Inhibition of Na^+/H^+ exchanger isoform 1 is neuroprotective in neonatal hypoxic ischemic brain injury. Antioxid Redox Signal. 2011; 14(10):1803–1813. [PubMed: 20712402]
14. Mujsce DJ, Christensen MA, Vannucci RC. Cerebral blood flow and edema in perinatal hypoxic-ischemic brain damage. Pediatr Res. 1990; 27(5):450–453. [PubMed: 2345670]
15. Shi Y, Chanana V, Watters JJ, Ferrazzano P, Sun D. Role of sodium/hydrogen exchanger isoform 1 in microglial activation and proinflammatory responses in ischemic brains. J Neurochem. 2011; 119(1):124–135. [PubMed: 21797866]
16. Denker SP, Ji S, Dingman A, Lee SY, Derugin N, Wendland MF, Vexler ZS. Macrophages are comprised of resident brain microglia not infiltrating peripheral monocytes acutely after neonatal stroke. J Neurochem. 2007; 100(4):893–904. [PubMed: 17212701]
17. Stevens SL, Bao J, Hollis J, Lessov NS, Clark WM, Stenzel-Poore MP. The use of flow cytometry to evaluate temporal changes in inflammatory cells following focal cerebral ischemia in mice. Brain Res. 2002; 932(1–2):110–119. [PubMed: 11911867]
18. Campanella M, Sciorati C, Tarozzo G, Beltramo M. Flow cytometric analysis of inflammatory cells in ischemic rat brain. Stroke. 2002; 33(2):586–592. [PubMed: 11823674]
19. Rezaie P. Microglia in the human nervous system. Neuroembryology and Aging. 2003; 2(1):14.
20. Verney C, Monier A, Fallet-Bianco C, Gressens P. Early microglial colonization of the human forebrain and possible involvement in periventricular white-matter injury of preterm infants. J Anat. 2010; 217(4):436–448. [PubMed: 20557401]

21. Sierra A, Encinas JM, Deudero JJ, Chancey JH, Enikolopov G, Overstreet-Wadiche LS, Tsirka SE, Maletic-Savatic M. Microglia shape adult hippocampal neurogenesis through apoptosis-coupled phagocytosis. Cell Stem Cell. 2010; 7(4):483–495. [PubMed: 20887954]
22. Jensen MB, Gonzalez B, Castellano B, Zimmer J. Microglial and astroglial reactions to anterograde axonal degeneration: A histochemical and immunocytochemical study of the adult rat fascia dentata after entorhinal perforant path lesions. Exp Brain Res. 1994; 98(2):245–260. [PubMed: 8050511]
23. Hailer NP, Grampp A, Nitsch R. Proliferation of microglia and astrocytes in the dentate gyrus following entorhinal cortex lesion: A quantitative bromodeoxyuridine-labelling study. Eur J Neurosci. 1999; 11(9):3359– 3364. [PubMed: 10510203]
24. Rappert A, Bechmann I, Pivneva T, Mahlo J, Biber K, Nolte C, Kovac AD, Gerard C, Boddeke HW, Nitsch R, Kettenmann H. Cxcr3-dependent microglial recruitment is essential for dendrite loss after brain lesion. J Neurosci. 2004; 24(39):8500–8509. [PubMed: 15456824]
25. Bechmann I, Goldmann J, Kovac AD, Kwidzinski E, Simburger E, Naftolin F, Dirnagl U, Nitsch R, Priller J. Circulating monocytic cells infiltrate layers of anterograde axonal degeneration where they transform into microglia. FASEB J. 2005; 19(6):647–649. [PubMed: 15671154]
26. Ladeby R, Wirenfeldt M, Dalmau I, Gregersen R, Garcia-Ovejero D, Babcock A, Owens T, Finsen B. Proliferating resident microglia express the stem cell antigen cd34 in response to acute neural injury. Glia. 2005; 50(2):121–131. [PubMed: 15657941]
27. Wirenfeldt M, Babcock AA, Ladeby R, Lambertsen KL, Dagnaes-Hansen F, Leslie RG, Owens T, Finsen B. Reactive microgliosis engages distinct responses by microglial subpopulations after minor central nervous system injury. J Neurosci Res. 2005; 82(4):507–514. [PubMed: 16237722]
28. Zhu C, Qiu L, Wang X, Xu F, Nilsson M, Cooper-Kuhn C, Kuhn HG, Blomgren K. Age-dependent regenerative responses in the striatum and cortex after hypoxia-ischemia. J Cereb Blood Flow Metab. 2009; 29(2):342–354. [PubMed: 18985054]
29. Carson MJ, Reilly CR, Sutcliffe JG, Lo D. Mature microglia resemble immature antigen-presenting cells. Glia. 1998; 22(1):72–85. [PubMed: 9436789]
30. Floris S, Blezer EL, Schreibelt G, Dopp E, van der Pol SM, Schadee-Eestermans IL, Nicolay K, Dijkstra CD, de Vries HE. Blood-brain barrier permeability and monocyte infiltration in experimental allergic encephalomyelitis: A quantitative mri study. Brain. 2004; 127(Pt 3):616–627. [PubMed: 14691063]
31. Qiao M, Malisza KL, Del Bigio MR, Tuor UI. Correlation of cerebral hypoxic-ischemic t2 changes with tissue alterations in water content and protein extravasation. Stroke. 2001; 32(4):958–963. [PubMed: 11283397]
32. Sheldon RA, Sedik C, Ferriero DM. Strain-related brain injury in neonatal mice subjected to hypoxia-ischemia. Brain Res. 1998; 810(1–2):114–122. [PubMed: 9813271]
33. Lafemina MJ, Sheldon RA, Ferriero DM. Acute hypoxia-ischemia results in hydrogen peroxide accumulation in neonatal but not adult mouse brain. Pediatr Res. 2006; 59(5):680–683. [PubMed: 16627881]
34. Mesples B, Plaisant F, Gressens P. Effects of interleukin-10 on neonatal excitotoxic brain lesions in mice. Brain Res Dev Brain Res. 2003; 141(1–2):25–32.
35. Yenari MA, Xu L, Tang XN, Qiao Y, Giffard RG. Microglia potentiate damage to blood-brain barrier constituents: Improvement by minocycline in vivo and in vitro. Stroke. 2006; 37(4):1087–1093. [PubMed: 16497985]
36. Li J, Baud O, Vartanian T, Volpe JJ, Rosenberg PA. Peroxynitrite generated by inducible nitric oxide synthase and nadph oxidase mediates microglial toxicity to oligodendrocytes. Proc Natl Acad Sci U S A. 2005; 102(28):9936–9941. [PubMed: 15998743]
37. Flavin MP, Coughlin K, Ho LT. Soluble macrophage factors trigger apoptosis in cultured hippocampal neurons. Neuroscience. 1997; 80(2):437–448. [PubMed: 9284347]
38. Butovsky O, Ziv Y, Schwartz A, Landa G, Talpalar AE, Pluchino S, Martino G, Schwartz M. Microglia activated by il-4 or ifn-gamma differentially induce neurogenesis and oligodendrogenesis from adult stem/progenitor cells. Mol Cell Neurosci. 2006; 31(1):149–160. [PubMed: 16297637]

39. Walton NM, Sutter BM, Laywell ED, Levkoff LH, Kearns SM, Marshall GP 2nd, Scheffler B, Steindler DA. Microglia instruct subventricular zone neurogenesis. Glia. 2006; 54(8):815–825. [PubMed: 16977605]

40. Olah M, Amor S, Brouwer N, Vinet J, Eggen B, Biber K, Boddeke HW. Identification of a microglia phenotype supportive of remyelination. Glia. 2012; 60(2):306–321. [PubMed: 22072381]

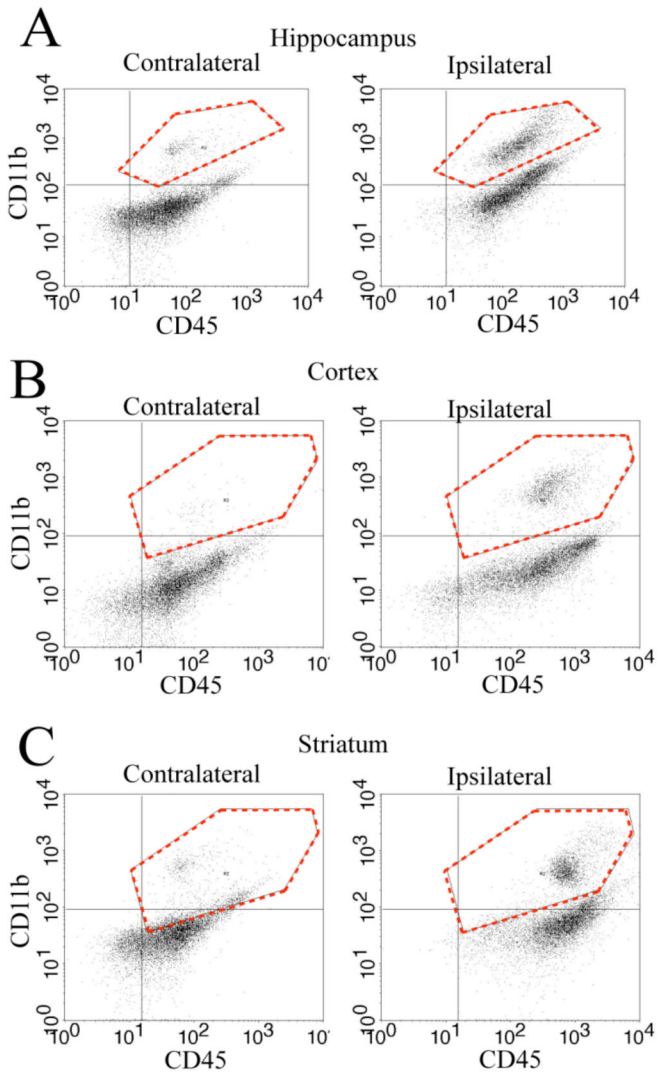

Figure 1. HI triggers accumulation of microglia/macrophage in P9 ischemic brains

A–C. Representative flow cytometry scatter plots of $CD11b^+/CD45^+$ cells in different brain regions (hippocampus, cortex, and striatum). Data were collected from the contralateral (CL) and ipsilateral (IL) hemispheres in P9 mice at 2 days post-HI (A) or 9 days post-HI (B; C). Y-axis: number of $CD11b^+$ cells. X-axis: number of $CD45^+$ cells. Dashed red line in the upper right quadrants: $CD11b^+/CD45^+$ cell population gated for further analysis in Figure 2–3.

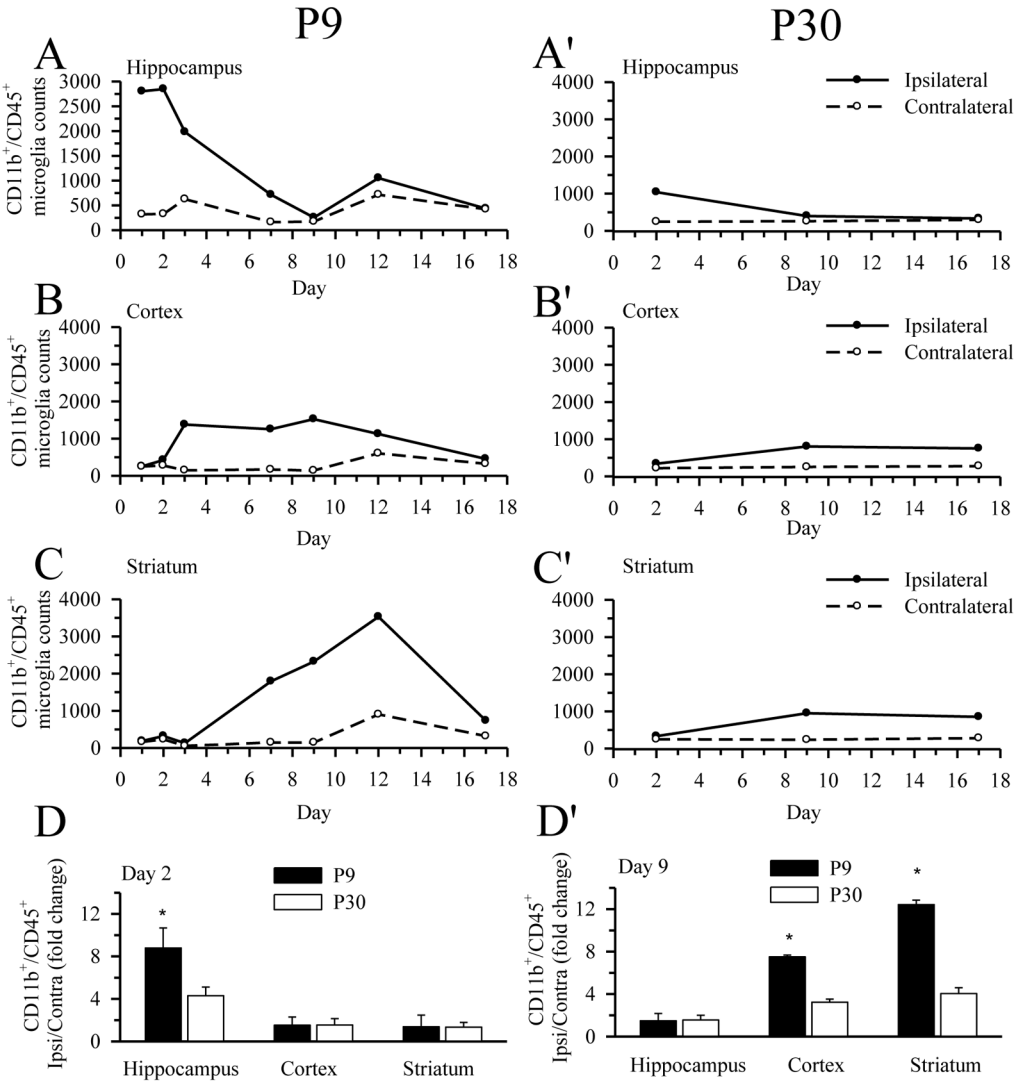

Figure 2. Comparison of microglia/macrophage activation in P9 and P30 brains after HI

The number of $CD11b^+/CD45^+$ microglia/macrophage in hippocampus, cortex, or striatum was analyzed at day 1–17 post-HI via flow cytometry. **A–D**: P9 brains. **A′– D′**: P30 brains. The relative change of microglia/macrophage in the three brain regions of the ipsilateral hemisphere was normalized with the contralateral hemispheres (**D** and **D′)**. Brain samples were pooled for this analysis (five animals for P9 and four animals for P30). Values are expressed as mean (A–C, A′– C′) and mean ± S.D. (D, D′), n = 3–4. * = $p < 0.05$ vs corresponding P30.

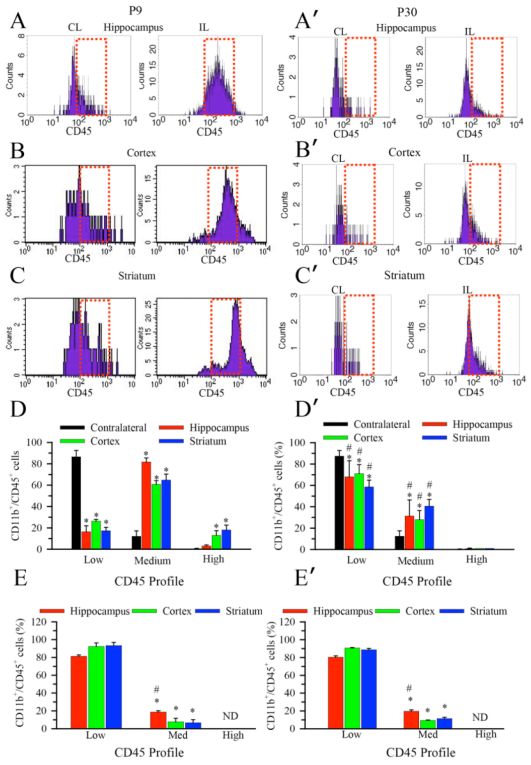

Figure 3. Selective elevation of CD45$^+$ expression in microglia/macrophage of P9 brains after HI

Representative FACS plots showing HI triggered selective elevation of CD45 expression in the CD11b$^+$/CD45$^+$ microglia from the ipsilateral hippocampus, cortex, and striatum in P9 mice. **A–D**: P9 brains. **A′–D′**: P30 brains. Data were collected at the peak level of the microglial activation in each brain region (day 2 post-HI for hippocampus, day 9 post-HI for cortex and striatum). Dotted red box: CD45 medium expression histograms. Expression of CD45 in the CD11b$^+$ microglial cells in P9 brains shifted from a low (<10^2) to medium (10^2–10^3) or higher level (> 10^3) after HI (reflected in the right shifted, broadened histogram curve). The proportion of the CD11b$^+$/CD45$^+$ cell population with low, medium, and high CD45 expression in each brain region are shown for P9 **(D)** and P30 **(D′)** mice. Values are expressed as mean ± S.D. (n = 3). * = $p < 0.05$ vs corresponding contralateral. # = $p < 0.05$ vs. corresponding P9. **E. E′.** The proportion of the CD11b$^+$/CD45$^+$ cell population with low, medium, and high CD45 expression in each brain region from naïve P9 (**E**) and P30 (**E′**) mice.. **ND**: not detectable. Values are expressed as mean ± S.D., n = 3. * = $p < 0.05$ vs. corresponding low, # = $p < 0.05$ vs. either corresponding cortex or striatum.

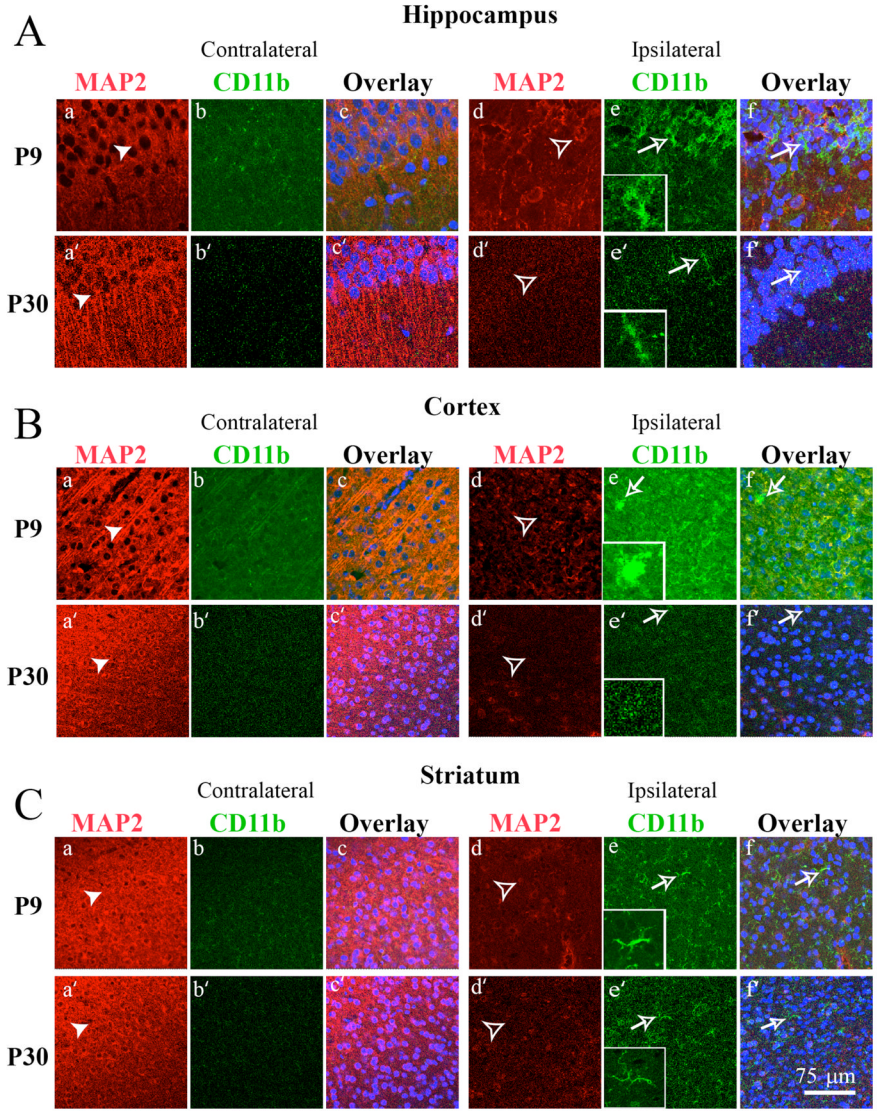

Figure 4. Immunostaining analysis of HI-mediated microglia/macrophage activation in the hippocampus, cortex and striatum of P9 and P30 brains

Double immunostaining of CD11b and MAP2 proteins were examined in the CA1 region of the hippocampus (**A**), the cortex (**B**) and the striatum (**C**) of the contralateral and ipsilateral hemispheres of P9 (top panels) and P30 brains (bottom panels) at 2 days following HI. Neurons were stained for MAP2 (red) in **A (a, a′, d, d′); B (a, a′, d, d′); C (a, a′, d, d′).** Microglia were stained for CD11b (green) in **A (b, b′, d, d′); B (b, b′, d, d′); C (b, b′, d, d′)**. Nuclei were stained with ToPro3 (blue) in the overlay images in **A–C** (**e, f, e′, f′**). The left column of panels is contralateral while the right column of panels is ipsilateral. Inset: magnified image. Scale bar: 75 μm. Arrow head: neurons with abundant MAP2 expression. Open arrowhead: loss of MAP2 expression. Open arrow: a reactive phenotype of microglia with short, stout processes and intense CD11b staining.

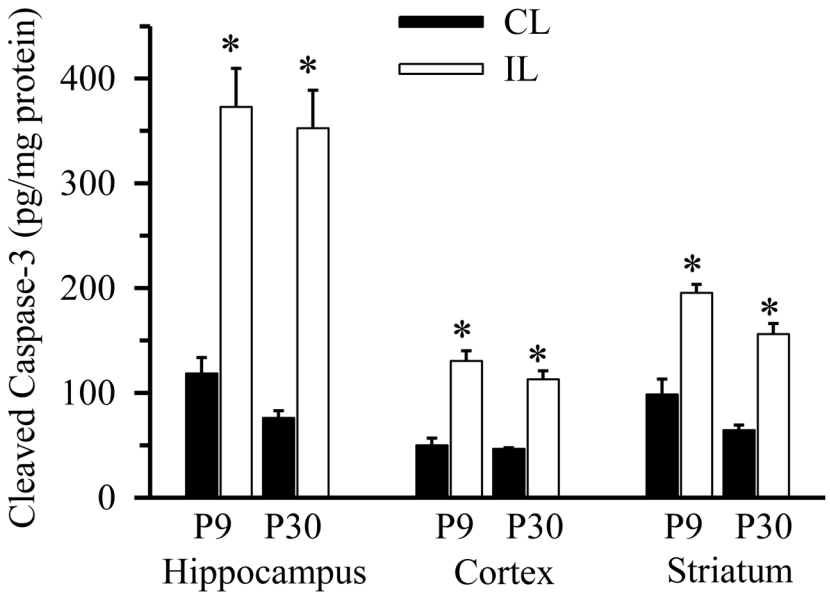

Figure 5. HI triggers apoptosis in P9 and P30 brains

Cleaved caspase-3 was determined via ELISA in hippocampus (H), cortex (C), and striatum (S) from contralateral (CL) and ipsilateral hemispheres (IL) of P9 and P30 brains 24 hours following HI. Cleaved caspase-3 content are expressed in picograms per milligram protein (pg/mg). Data are mean ± SD, n = 3, * $p < 0.05$ vs. corresponding CL hemisphere.

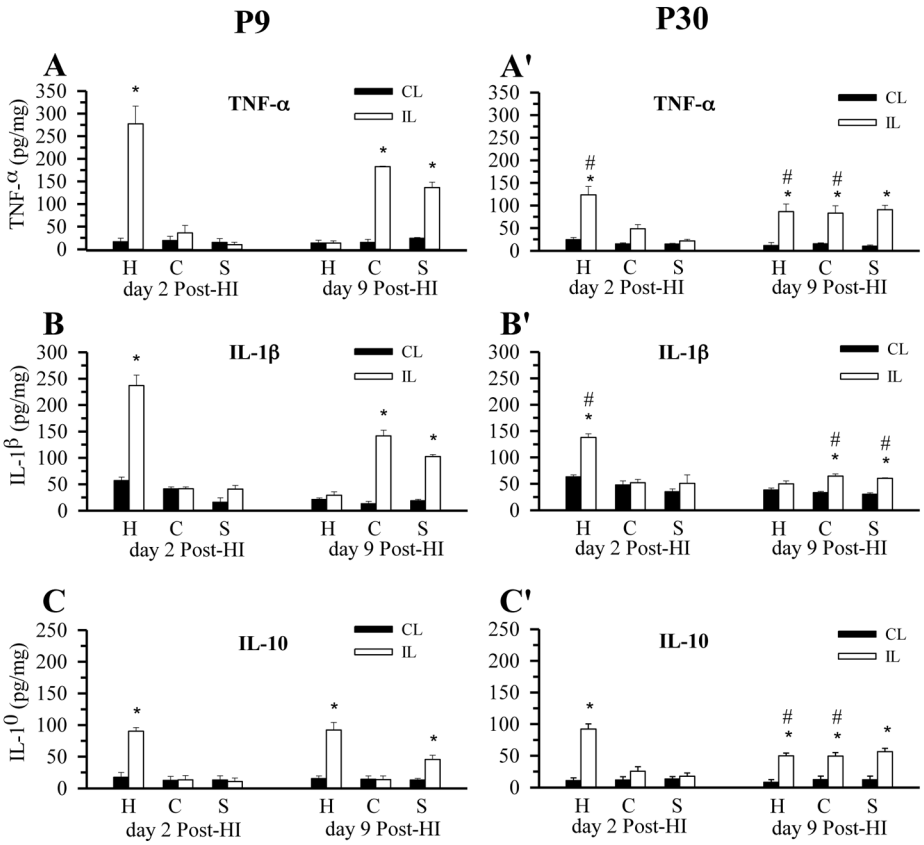

Figure 6. HI selectively triggers pro-inflammatory cytokine expression in P9 brains

TNF-α, IL-1β, and IL-10 in hippocampus (H), cortex (C), and striatum (S) in contralateral and ipsilateral hemispheres were determined via ELISA. **A–C**: P9 brains (day 2 post-HI and day 9 post-HI). **A′– C′**: P30 brains (day 2 post-HI and day 9 post-HI). Cytokine content are expressed in picograms per milligram protein (pg/mg). Data are mean ± SD, n = 3, * $p < 0.05$ vs. corresponding contralateral hemisphere; # $p > 0.05$ ipsilateral P30 vs. corresponding ipsilateral P9.